Model-based optimization of field-scale electrokinetic remediation of marine sediments

Matteo Masi [a], Alessio Ceccarini [b], Renato Iannelli [a]
[a] University of Pisa, Department of Energy, Systems, Land and Construction Engineering (Italy)[1],
[b] University of Pisa, Department of Chemistry and Industrial Chemistry (Italy)

Abstract

This work presents a model-based approach for the optimization of electrokinetic remediation of porous media at the field scale. We developed a numerical model to simulate transport and reactions occurring during electric field application. The model was applied to the case study of a 150 m^3 pilot scale electrokinetic plant treating heavy metal-contaminated marine sediments, in order to evaluate the influence of the design parameters on treatment efficiency and costs. The numerical model consisted of a transport model able to simulate electromigration and electroosmosis coupled with a geochemical model, which calculates aqueous speciation, precipitation-dissolution, adsorption and surface complexation reactions. Laboratory-scale experiments were carried out to calibrate and validate the model. The validated model was used to carry out a parametric study in order to calculate the treatment costs as a function of the parameters considered. The analysis allowed us to identify the optimum set of parameters which minimized the costs.

Keywords: numerical model; cost estimation; optimization; dredged sediments; heavy metals

1. Introduction

Sediments deriving from dredging activities in harbours and coastal areas are often affected by several hazardous pollutants, mainly heavy metals and hydrocarbons. In most cases, pollution is caused by long-term accumulation due to activities within the harbours, such as navigation, industry, drainage, etc. Contaminated sediments cannot be dumped into open sea or reused; the most common options for their management is their disposal into confined disposal facilities or into landfills. The considerable amount of sediments dredged periodically to maintain water depths adequate for navigational purposes, generates significant environmental impacts and high costs.

The remediation of long-term polluted marine sediment is particularly critical because they are often characterized by features that make pollution mobilization more challenging such as low hydraulic permeability, high salinity and strong acid-neutralizing capacity due to high presence of organic matter and carbonates [1].

In marine sediment remediation, heavy metal pollution is a major issue because most sediments consist of clay minerals and organic matter. Metals can be bound to clay surfaces or complexed with organic matter thus reducing their mobility through the porous matrix [2].

In this context, electrokinetic remediation (EKR) is widely recognised as an efficient technique for addressing the abovementioned issues [3–5]. Metals can be present as soluble ions, or as oxides, hydroxides, carbonates, sulphates or other organic and inorganic complexes bound to sediment

---

particles. Consequently, they can be directly mobilized from the sediment matrix as long as they are present in ionic forms or bound to mobile polar complexes. Several possible enhancement strategies are adopted in order to induce favourable pH conditions and/or interacting with heavy metals with the aim to reduce remediation time and costs [6]. One option is to exploit the acid front migrating from the anode as the consequence of the acidic conditions due to electrolysis reaction at the anode. The progressive acidification of the sediment facilitates the solubilisation of metals. Once dissolved, metals are transported toward the electrodes reaching the electrolytes; metals can be subsequently removed from the electrolyses by appropriate treatment of the liquid phase.

The electric field application causes transport mechanisms (electromigration, electroosmosis and electrophoresis), electrode reactions and geochemical reactions occurring at the same time. The whole system is characterized by a strongly non-linear and transient behaviour [7]. Moreover, the time scale at which the various mechanisms occur is different. Therefore, their prediction is often a complex task, especially if carried out only on an experimental basis. Especially in the case of sediments with high buffering capacity, remediation times may be extended significantly (by several months, if not years). In these cases, the mere laboratory experiments would require excessive time and modelling represents an indispensable tool for the identification of the main parameters that influence the efficiency of treatment and for the prediction of contaminant removal efficiencies. In addition to allowing identification of the main factors that determine the correct outcome of remediation, a mathematical model is also a useful tool for testing different operating configurations, design and operational parameters for an efficient implementation of the technology at full scale.

Many models have been proposed in literature for the simulation electrokinetic extraction of contaminants [8–11]. These models have been mainly applied to the simulation of experimental data obtained in the laboratory. Application at full scale is unusual [12,13] and even more rare is their use for engineering purposes [14].

This paper presents a numerical model for the optimization of in situ electrokinetic processes, including the ability to estimate optimal design parameters. The model simulates the transport processes and chemical reactions. The model was applied to the case study of a pilot plant built within the European project Life+ "SEKRET" ("ElectroKinetic Sediment Remediation Technology for heavy metal pollution removal"), for the treatment of 150 m^3 dredged sediments contaminated by heavy metals. A parametric study was carried out to evaluate the sensitivity of treatment efficiency to sediment properties and the distance between the electrodes, in order to identify the optimum set of parameters that minimizes the treatment costs.

2. Materials and methods

2.1. Model

The physico-chemical model couples the electrokinetic transport and chemical reactions by the Nernst-Planck equation:

$$n \frac{\partial c_i}{\partial t} = -\nabla \cdot \left[-D_i^* \nabla c_i - (U_i^* + k_{eo}) c_i \nabla \phi \right] + n R_i \tag{1}$$

where i denotes the i-th species, n the porosity, D_i^* (m^2 s^{-1}) the effective diffusion coefficient of the i-th specie, c_i (mol m^{-3}) the concentration of the i-th specie, U_i^* (m^2 s^{-1} V^{-1}) the effective ion mobility, ϕ (V) the electric potential, k_{eo} (m^2 V^{-1} s^{-1}) the coefficient of electroosmotic permeability and R_i (mol m^{-3} s^{-1}) represents a volumetric net source or sink of c_i due to chemical reactions. The effective diffusion coefficient and effective ion mobility in Equation (1) were defined as:

$$D_i^* = n\tau D_i \quad , \quad U_i^* = n\tau U_i \tag{2}$$

where D_i (m^2 s^{-1}) and U_i (m^2 s^{-1} V^{-1}) are the diffusion coefficient and ion mobility at infinite dilution, respectively, and τ the tortuosity.

The Nernst-Townsend-Einstein relation [15] was applied to relate diffusivity to ionic mobility.

We made a number of assumptions to simplify the formulation: we neglected advective flow because of its lower order of magnitude compared to electroosmotic flow due to low hydraulic permeability of the investigated material; we assumed that the porous medium is saturated and isotropic; the pore geometry characteristics (e.g. porosity, tortuosity) were assumed to stay unchanged over time; electrophoresis was neglected, since colloid migration is mostly hindered by the immobile phase of the sediment.

To simulate the reactions taking place during electric field application, we selected a set of phenomena that were recognized as the most important factors in electrokinetic remediation of marine sediments [4]. Specifically, they were: (1) water electrolysis at the electrodes, (2) acid neutralization capacity, (3) adsorption/desorption of contaminants, (4) aqueous speciation (i.e. formation of complexes), and (5) precipitation/dissolution of species.

The acid-buffering capacity of sediments was modelled as a generalized surface complexation reaction [16]:

$$\equiv SOH + H^+ \rightleftharpoons \equiv SOH_2^+ \tag{3}$$

$$\equiv SOH \rightleftharpoons \equiv SO^- + H^+ \tag{4}$$
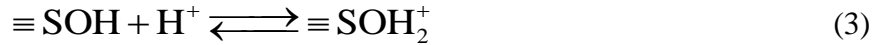
where $\equiv$SOH represent an active site and S is a metal associated to the solid structure and located at the solid-liquid interface.

The sorption and desorption of the investigated heavy metals onto particle surfaces were modelled as linear adsorption isotherms.

The aqueous formation of complexes, precipitation and dissolution reactions were calculated using the PHREEQC code. Equations representing these reactions are not reported here, as they can be found in [17].

Transport processes and chemical reactions were implemented using a two-steps sequential non-iterative split-operator scheme, under the assumption of local chemical equilibrium. In the first step, diffusion, electromigration and electroosmosis are integrated with finite element method. In the second step, chemical reactions are calculated with PHREEQC code.

2.2. Case study

The research activities reported in the present work were carried out in the framework of the Life+ project LIFE12 ENV/IT/442 "SEKRET" ("Sediment electrokinetic remediation technology for

heavy metal pollution removal"), which is supported financially by the European Commission from 2013 to 2017. The project, which is ongoing at the time of this writing, aims to demonstrate the applicability of electrokinetic technology for the remediation of dredged marine sediments contaminated by heavy metals. The project involved the construction of an ex-situ demonstration plant in a dedicated area in the port of Livorno (Italy) for the treatment of 150 m^3 of sediment dredged from the port seabed. The investigated metals are Cd, Cr, Pb, Ni, Zn, As and Cu. The design of the ex-situ plant started in 2013 and the plant was operative in July 2015. The remediation, which is expected to last 18 months, is currently ongoing.

The plant consists of the following parts: a treatment basin containing the sediments, with a system of wells and pipes for electrode installation and electrolyte circulation; electrical units for the application of the electric field to the sediment; an electrolyte management system for catholyte and anolyte pH control; a gas scrubbing system the abatement of chlorine gas; a reverse osmosis (RO) section for the control of the salinity of the electrolytes; a monitoring and control system.

Pictures of the treatment basin are shown in Figure 1. The electric field is applied by means of arrays of anodes and cathodes installed inside vertical slotted wells (PVC slotted pipes) in the sediment. Electrodes having the same polarity are spaced about 1.1 m. The distance between anode and cathode is 1 m. The number of electrodes is 84 (42 anodes and 42 cathodes). A current density of 4–5 A/m^2 is applied 24 hours a day, seven days a week. The operating pH is approximately pH $\approx$ 3 for catholyte and pH $\approx$ 2 for anolyte. Nitric acid is added at the catholyte to maintain the set-point pH.

Figure 1. Left: filling of the basin with dredged sediments (February 2015). Right: plant installation completed (April 2015).

2.3. Sediment characterization

The sediment was dredged from an area in the harbour which had been previously classified as highly polluted by heavy metals. The volume of dredged material for the demonstration plant was 150 m^3. After conveying the material to the treatment facility, samples were taken from the basin from various locations at different heights. A representative sample was prepared by homogenizing all the collected samples. The samples were oven-dried at 105 °C and sieved to remove the 2 mm oversized particulate matter. When required by the analytical procedures, oven-drying was performed at 60 °C so as to prevent any loss of volatile material.

The pH was measured according to ISO 10390:2005. The acid buffering capacity was determined by titration method using 0.1 M HCl. The grain size distribution was determined according to ICRAM reference methods (2001), data sheet number 3 —"grain size characteristics". Sediment

electrical conductivity was determined with 4-electrode method in a cylindrical sample holder using AC current injection. TOC was measured according to the standard methods issued by the Italian Ministry of Agriculture and Forests. CEC was determined according to ISO 11260:1994 method. Metal content was determined using either atomic absorption spectrometry (US EPA 7000B 2007) or ICP-OES (US EPA 6010C 2007). Acid digestion of the sediments was performed in accordance with the US EPA 3050B 1996 method, while acid digestion of aqueous samples was performed according to US EPA method 3010A.

3. Results and discussion

3.1. Sediment characterization

The physicochemical properties of the sediments are presented in Table 1.

Table 1. Physicochemical properties of the sediments. pH, particle size distribution and chemical analysis were applied to three replicate samples.

Physico-chemical properties	
pH	8.5 ± 0.17
Electrical resistivity	0.63 ± 0.12 Ωm
Porosity	0.48 ± 0.07
Hydraulic conductivity	3.5×10^{-10} m/s
Cation exchange capacity (CEC)	11 meq/100 g
Total organic carbon (TOC)	< 1 %
Grain size distribution	
d > 2 mm	0 %
0.063 < d < 2 mm	49.4 ± 2.9 %
d < 0.063 mm	50.6 ± 2.9 %
Heavy metal content (mg/kg)	
As	14.3 ± 1.4
Cd	2.0 ± 0.9
Cr(tot)	51.0 ± 5.1
Ni	38.8 ± 3.9
Pb	27.6 ± 4.6
Cu	55.1 ± 5.1
Zn	112.2 ± 6.5

3.2. Model setup

In order to reproduce the geometrical arrangement of the wells and the electrodes of the pilot plant, a simplified 2D schematization was built, which reproduces the actual 3D electric field spatial distribution, assuming that the variation of the vertical direction electric field can be neglected. The validity of this hypothesis was demonstrated by a comparison of the simulated electric field and electric field measured in situ [18].
The model domain consisted of a 2D closed domain, which was discretized into a number of finite elements variable in the range 836 to 4470, depending on the case simulated. The boundary conditions at the electrodes were defined at the outer edge of the wells. In this study, we considered the only transportation of lead, which has been considered as representative metal [19]. The model

included the main complexes forming in the working conditions: Pb^{2+}, $PbCl^+$, $PbCl_3^-$, $PbCl_4^{2-}$, $PbCl_2$, $PbNO_3^+$ e $Pb(NO_3)_2$. Finally, six other major species were included in the model: H^+, OH^-, Na^+, Cl^-, NO_3^-. The model also calculated the formation and dissolution of solid phases (e.g., $Pb_3(OH)_2(CO_3)_2$).

At the electrodes, H^+ (anode) and OH^- (cathode) fluxes were calculated using Faraday's law of electrolysis. For example, the H^+ flux J_{H+} (mol m^{-2} s^{-1}) was calculated as $J_{H+} = J / F$, where J (A m^{-2}) represents the current density on the boundary surface (half of the edge of the electrode wells). 100% Faraday efficiency was assumed for water electrolysis at the electrodes. At the cathode, the flux of NO_3^- was assumed as a boundary condition instead of OH^- flux, because OH^- ions are being neutralized by nitric acid addition and replaced by NO_3^-.

The boundary conditions for the other elements were: constant concentrations at both anolyte and catholyte for Na^+, Cl^- and NO_3^-; zero concentration of Pb at both electrolytes, including Pb complexes.

Model parameters were either calibrated using measured values or taken from Masi et al., 2017 [19]. The coefficient of electroosmotic permeability was set to -2×10^{-9} m^2 s^{-1} V^{-1}; the value is negative because reverse electroosmotic flow (i.e., from cathode to anode) occurs when nitric acid is used as enhancing agent, as observed in the cited reference. Electrode voltage and current values were adjusted case-by-case.

3.3. Numerical simulation results

Simulations were carried out in order to evaluate acid front and lead migration in the same conditions as those adopted in the case study. The results are shown in Figure 2.
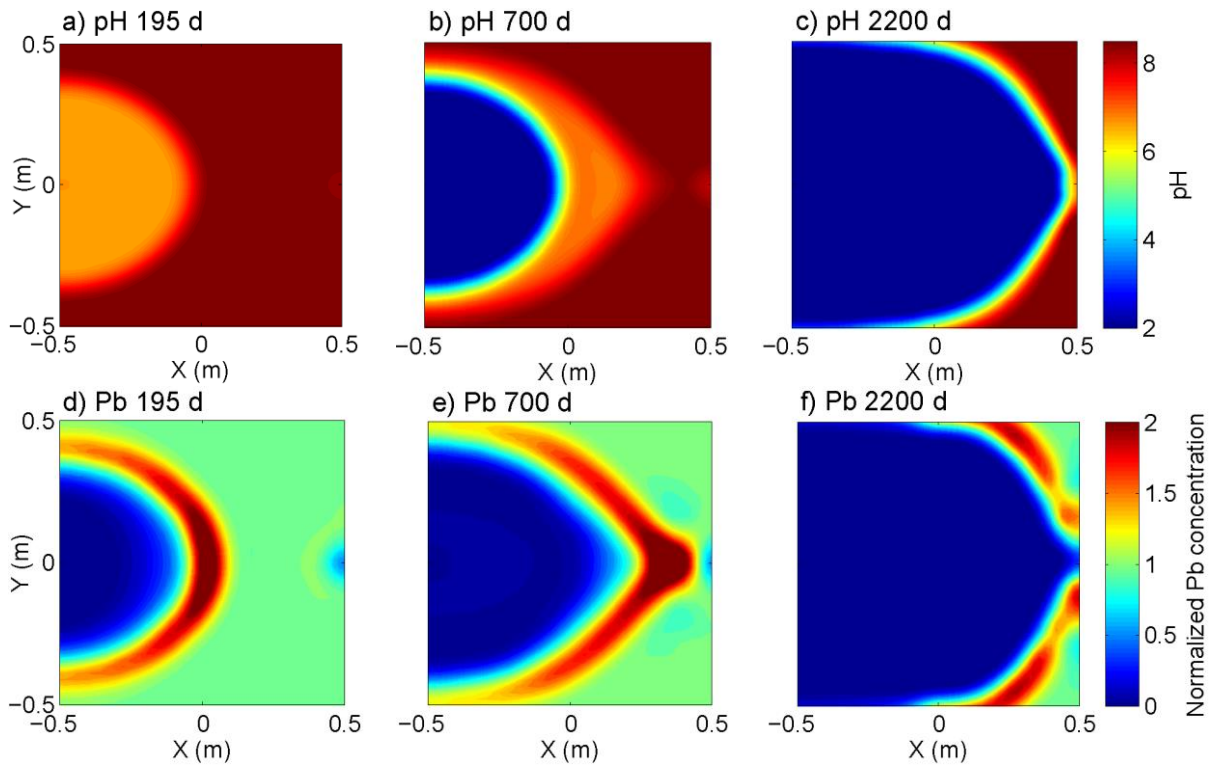
Figure 2. 2D model results. (a–c) pH distribution and (d–f) residual lead concentration after 195, 700 and 2200 days.

The figure shows the pH and residual lead distributions as a function of remediation time. The advance of the acid front from the anode to the cathode (Figure 5c) was faster along the anode-cathode axis because in this region the electric field strength was higher than at the borders of the domain. As a result, residual lead concentration followed the same trend and higher transport rates were observed along the anode-cathode line.

The figure also shows that accumulation of lead occurred in a narrow zone of the domain and moved toward the cathode with time. This zone corresponded to the areas where pH transition was sharp, jumping from acidic to alkaline conditions (pH ≈ 7-8), which led to precipitation of Pb.

3.4. Model-based parameter optimization

Various sets of simulations were carried out by varying two main parameters: the distance between the electrodes and the buffering capacity of the sediment. The buffering capacity is here defined as the equivalent amount of H^+ ions needed to decrease the pH of the sediment to pH = 3 . While the distance between electrodes may be considered as the main design parameter, the buffering capacity is related to the intrinsic physical-chemical characteristics of the sediment; this parameter then, while not being changeable arbitrarily, however, it allowed us to evaluate the sensitivity of treatment costs to its values. The parameters used in the simulations were as follows: a target Pb removal of 70%, a constant resistivity of 1 Ωm, a constant power output of 100 Wm⁻³, depreciation of 20% for costs related to the electrodes, assuming that the latter can be reused in other applications. The results of the parametric study are shown in Figure 3. In the graph on the left shows estimates of retail costs as a function of anode-cathode distance. To the right, the graph shows the total cost, calculated as the sum of the individual costs, in each case depending on the buffering capacity of the sediment, showing that the latter is a feature that will greatly influence the total cost of treatment. In the same graph, the minimum points show how the choice of the optimal distance between the electrodes is unique, given the characteristics of the sediment.
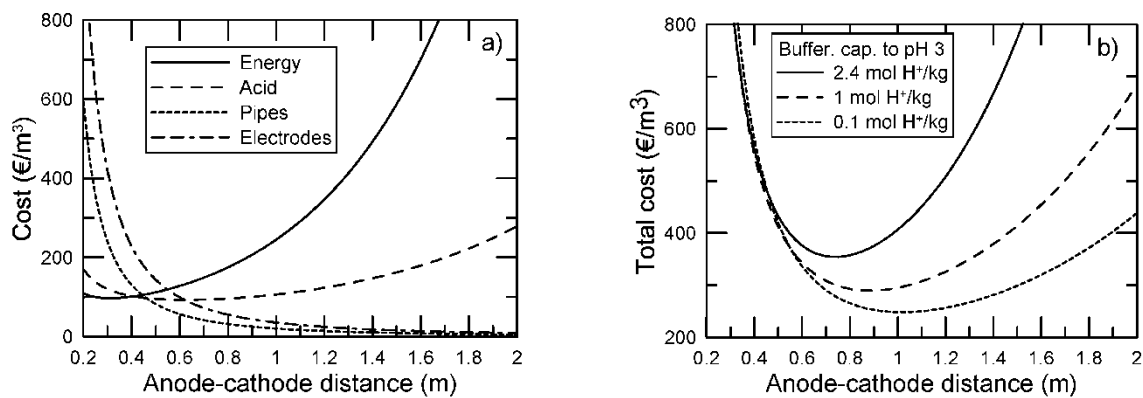

Figure 3. (a) Estimated costs for energy, acid, pipes and electrodes for the reference case (buffering capacity 2.4 mol H^+/kg). (b) Curves of total cost.

A point of minimum can be clearly identified for each curve. The locations of these points are dependent on sediment buffering capacity. The point of minimum shifts toward larger electrode

distances with decreasing buffering capacity. For instance, the optimum electrode distance calculated for the reference case was approximately 0.75 m, while it increases to 0.88 m and 1 m in the case of 1 mol H^+/kg and 0.1 mol H^+/kg, respectively.

It should be pointed out that the presented cost analysis was significantly simplified compared to cost estimation as typically performed during project implementation stage. However, the cost analysis can be extended to integrate all other costs not included in the present treatise, independently from simulation results.

4. Conclusions

We developed a two-dimensional numerical model to simulate transport phenomena and chemical reactions taking place during electrokinetic remediation of porous media contaminated by heavy metals. The model was applied to the case study of the "SEKRET" remediation plant, which treats 150 m^3 marine sediments dredged from the port of Livorno (Italy). After the model was calibrated and validated, a parametric study was performed, which allowed us to obtain cost curves as a function of the main operating parameters and the characteristics of the sediment. The curves, calculated from the results of numerical simulations, allowed to identify the optimum set of parameters that minimized the treatment costs.

In conclusion, we strongly believe that the methodology and the results obtained can be used as a valuable tool for the design and optimization of in situ electrokinetic treatment systems.

References

[1] C.N. Mulligan, M. Fukue, Y. Sato, Sediments contamination and sustainable remediation, CRC Press, 2009.

[2] J.-F. Peng, Y.-H. Song, P. Yuan, X.-Y. Cui, G.-L. Qiu, The remediation of heavy metals contaminated sediment., J. Hazard. Mater. 161 (2009) 633–40. doi:10.1016/j.jhazmat.2008.04.061.

[3] A. Colacicco, G. De Gioannis, A. Muntoni, E. Pettinao, A. Polettini, R. Pomi, Enhanced electrokinetic treatment of marine sediments contaminated by heavy metals and PAHs., Chemosphere. 81 (2010) 46–56. doi:10.1016/j.chemosphere.2010.07.004.

[4] R. Iannelli, M. Masi, A. Ceccarini, M.B. Ostuni, R. Lageman, A. Muntoni, et al., Electrokinetic remediation of metal-polluted marine sediments: experimental investigation for plant design, Electrochim. Acta. 181 (2015) 146–159. doi:10.1016/j.electacta.2015.04.093.

[5] K.-J. Kim, D.-H. Kim, J.-C. Yoo, K. Baek, Electrokinetic extraction of heavy metals from dredged marine sediment, Sep. Purif. Technol. 79 (2011) 164–169. doi:10.1016/j.seppur.2011.02.010.

[6] A.T. Yeung, Y.-Y. Gu, A review on techniques to enhance electrochemical remediation of contaminated soils., J. Hazard. Mater. 195 (2011) 11–29. doi:10.1016/j.jhazmat.2011.08.047.

[7] A.N. Alshawabkeh, Electrokinetic Soil Remediation: Challenges and Opportunities, Sep. Sci. Technol. 44 (2009) 2171–2187. doi:10.1080/01496390902976681.

[8] A. Al-Hamdan, K. Reddy, Electrokinetic Remediation Modeling Incorporating Geochemical Effects, J.

Geotech. Geoenvironmental Eng. 134 (2008) 91–105. doi:10.1061/(ASCE)1090-0241(2008)134:1(91).

[9] S. Amrate, D.E. Akretche, Modeling EDTA enhanced electrokinetic remediation of lead contaminated soils., Chemosphere. 60 (2005) 1376–83. doi:10.1016/j.chemosphere.2005.02.021.

[10] J.M. Paz-García, M. Villén-Guzmán, A. García-Rubio, S. Hall, M. Ristinmaa, C. Gómez-Lahoz, A Coupled Reactive-Transport Model for Electrokinetic Remediation, in: A.B. Ribeiro, E.P. Mateus, N. Couto (Eds.), Electrokinet. Across Discip. Cont. SE - 13, Springer International Publishing, 2016: pp. 251–278. doi:10.1007/978-3-319-20179-5_13.

[11] J.-W. Yu, I. Neretnieks, Modelling of transport and reaction processes in a porous medium in an electrical field, Chem. Eng. Sci. 51 (1996) 4355–4368. doi:10.1016/0009-2509(96)00283-7.

[12] J.M. Paz-García, K. Baek, I.D. Alshawabkeh, A.N. Alshawabkeh, A generalized model for transport of contaminants in soil by electric fields, J. Environ. Sci. Heal. Part A. 47 (2012) 308–318. doi:10.1080/10934529.2012.640911.

[13] V. Rubio-Nieblas, M. Perez-tello, R.A. Jacobs, R. Herrera-Urbina, S.A. Moreno-Zazueta, Two-dimensional computational modeling of the electrokinetic remediation of a copper-contaminated soil part I: model validation, Dyna. 81 (2014). doi:10.15446/dyna.v81n183.36896.

[14] M.Z. Wu, D.A. Reynolds, A. Fourie, D.G. Thomas, Optimal Field Approaches for Electrokinetic In Situ Oxidation Remediation, Groundw. Monit. Remediat. 33 (2013) 62–74. doi:10.1111/j.1745-6592.2012.01410.x.

[15] A.N. Alshawabkeh, Y.B. Acar, Removal of contaminants from soils by electrokinetics: A theoretical treatise, J. Environ. Sci. Heal. . Part A Environ. Sci. Eng. Toxicol. 27 (1992) 1835–1861. doi:10.1080/10934529209375828.

[16] D.A. Dzombak, F.M.M. Morel, Surface complexation modeling: hydrous ferric oxide, John Wiley & Sons, 1990.

[17] B.D.L. Parkhurst, C. a J. Appelo, User's Guide To PHREEQC (version 2) — a Computer Program for Speciation, Batch-Reaction, One-Dimensional Transport and Inverse Geochemical Calculations, 1999. http://downloads.openchannelsoftware.org/PHREEQC/manual.pdf.

[18] M. Masi, Electrokinetic remediation of heavy metal-contaminated marine sediments: experiments and modelling, PhD dissertation. ISBN 978-88-90228-92-6. University of Pisa, 2017. doi:10.13131/unipi/etd/01122017-120456.

[19] M. Masi, A. Ceccarini, R. Iannelli, Multispecies reactive transport modelling of electrokinetic remediation of harbour sediments, J. Hazard. Mater. 326 (2017) 187–196. doi:10.1016/j.jhazmat.2016.12.032.